**Proceedings of the ASME 2025 44th International Conference on Ocean, Offshore and Arctic Engineering OMAE 2025
June 22–27, 2025, Vancouver, British Columbia, Canada**

OMAE2025-157366

DRAFT: LOW FIDELITY MODELING FOR THE PREDICTION OF LONG-TERM FLOATING OFFSHORE WIND TURBINE PERFORMANCE

Jackson Pilgrim Hardin[1,*], Federico Zilic de Arcos[1], Thomas A.A. Adcock[1], Emma C. Edwards[1],

[1]Department of Engineering Science, University of Oxford, Oxford, United Kingdom, OX1 3PH

ABSTRACT

Floating offshore wind energy has been identified as a critical source of future sustainable energy. This work is part of a broader effort to characterize the performance difference between floating and fixed offshore wind turbines. We characterize the discrepancy between low fidelity blade element momentum theory (BEMT) simulations and higher fidelity methods for floating turbines in the context of prescribed, harmonic platform motion. Five variations of a BEMT solver with varying empirical corrections are compared to fully blade resolved computational fluid dynamics simulations, as well as two experimental studies. BEMT's ability to predict rotor integrated parameters describing the mean and fluctuating components of power and thrust is analyzed. We then utilize the BEMT method to predict the mean and fluctuating component of rotor thrust and turbine power production under harmonic motion at frequencies of interest. The BEMT method predicts small variations in the mean components, but very large fluctuating components of power and thrust at representative platform natural frequencies. Additionally, power capture is predicted to increase at below rated wind speed and decrease at rated wind speed during motion.

Keywords: Floating offshore wind turbine, Blade element momentum theory, Performance prediction

1. INTRODUCTION

In this project we aim to understand how floating platform motion affects the performance of floating offshore wind turbines (FOWTs). In particular, we are interested in parameters that will drive design of future FOWT development projects, such as power coefficient (C_{P}), and rotor thrust coefficient (C_{T}). In this study we aim to characterize the effect of platform motion on FOWT performance by constructing motion-adjusted power and thrust curves for operational wind speeds. This analysis will be extended in future work to consider long-term FOWT performance in a variety of operational conditions, and therefore low fidelity numerical modeling techniques are necessary. As such, we also examine the applicability of this low fidelity modeling to FOWT dynamics.

A variety of platform designs for FOWTs have been developed each of which is prone to varying platform motion responses [1, 2]. As such, aerodynamic analysis of FOWTs must take into account this platform motion. High fidelity tools for the aerodynamic analysis of moving turbines such as blade resolved Reynolds averaged Navier-Stokes computational fluid dynamics (RANS-CFD) and actuator line computational fluid dynamics (ACL-CFD) models have demonstrated good accuracy in describing rotor and blade forces during operation. Tran and Kim [3] demonstrate a three dimensional, blade resolved, RANS-CFD model to predict thrust and torque fluctuation of the NREL 5 MW reference wind turbine during prescribed platform surge motion. Their model predicts variations in C_{P} and C_{T} of 0 to 1.3 and 0.13 to 1.19 respectively for motion of 8 m amplitude at 0.123 Hz. In this case, C_{P} and C_{T} are able to exceed one as they are normalized by the free stream velocity not the rotor experienced wind speed.

In addition, mid-fidelity models such as free vortex wake methods (FVM) have also shown success in FOWT modeling. Sebastian and Lackner [4] utilized a FVM model to predict thrust and power coefficients with less than 1.5 percent error compared to experimental results from the Energy Research Center of the Netherlands' MEXICO rotor. Lee and Lee [5] and Ramos-Garcia et al. [6] have also used FVM to model turbines in prescribed platform motion, predicting large variations in turbine performance under prescribed motion.

Despite their accuracy, these higher fidelity models can be orders of magnitude slower than the low fidelity blade element momentum theory (BEMT) [7]. BEMT has been the industry standard for wind turbine analysis for some time, being utilized by popular tools such as NREL's OpenFAST [8]. The BEMT model is a combination of blade element theory, which analyses a section of the turbine blade as a two-dimensional airfoil, and momentum theory, which analyses the macroscopic momentum balance of the working fluid across the rotor plane. The combination of these

*Corresponding author: Jackson.Hardin@oriel.ox.ac.uk

two theories is used to predict blade forces, power generation, and efficiency [9].

Apsley and Stansby [10] compared a BEMT solver to actuator line CFD, finding close agreement in power coefficient for all tip speed ratios and close agreement in thrust coefficients for all operational tip speed ratios. In addition, BEMT predicted turbine performance in oscillating flows with less than 15 % error relative to ACL-CFD. Multiple other authors [11–13] have also utilized BEMT to predict turbine performance in platform motion.

Although it is orders of magnitude less computationally expensive than some high fidelity methods, BEMT assumes quasi-steady flow conditions which may be violated during rapid motion of the rotor disk. Unsteady inflow conditions could occur during surge and pitch motion, common in FOWT operation, in which the rotor disk moves in and out of the incoming wind. To have confidence in its use for turbine design, BEMT analysis of FOWT platform motion must be carefully vetted and validated with experimental results or higher fidelity numerical methods.

Papi et al. [14] compared rotor thrust predicted by a BEMT model, a BEMT model with a dynamic correction meant to account for the changing inflow conditions caused by platform motion, a FVM model, and an ACL-CFD simulation. The authors show that BEMT both with and without the dynamic correction predicts turbine thrust with less than 10% difference compared to the higher fidelity methods at rated wind speeds with small to medium frequency motion. However, BEMT with or without dynamic correction fails to capture non-linear effects such as Lowry's returning wake problem or unsteady airfoil effects due to platform motion at frequencies greater than two or three times the rotor rotational speed. As such, the types of motion studied must be determined to be within the range of accurate BEMT analysis. Additionally, the errors and inaccuracies should be well understood in order to make sound engineering decisions.

In light of these challenges, we aim to validate the use of the low fidelity blade element momentum theory for the case of rotor motion. Specifically, we aim to validate its ability to predict the rotor-wide parameters important for FOWT design and economic feasibility described previously. Additionally, we must validate the method's ability to predict rotor thrust and the fluctuation of rotor thrust, as these play an important role in the system coupled aero-hydro dynamic force balance. Finally, we demonstrate the use of a low fidelity BEMT model to predict turbine performance under prescribed harmonic surge motion at frequencies of interest including platform natural frequencies as well as a representative wave frequency. This motion adjusted performance can be utilized to estimate the effect of platform motion on power performance or turbine blade loading to inform design decisions like platform type, as well as to understand the implications of selecting floating versus fixed turbine types.

2. METHODS

We elect to utilize an in-house implementation of blade element momentum theory to examine the effects of prescribed platform motion. Most current open source BEMT models have limited dynamic inflow modeling capacity, while the development of our own BEMT implementation allows for maximum flexibility in the selection of empirical corrections used in the model.

BEMT is derived from the combination of 1-D momentum theory and blade element theory. The theory assumes that the incoming flow is quasi-steady (the free stream velocity, blade pitch, and rotor rotational speed are constant), and that the rotor may be split into N equally spaced annuli within which the flow does not interact with any other annulus. The torque and thrust contribution of each annulus can be expressed through momentum theory as

$$\mathrm{d}Q = 4\pi r^3 \rho U_\infty \Omega (1-a) a' \mathrm{d}r, \tag{1}$$

$$\mathrm{d}T = 4\pi r \rho U_\infty^2 (1-a) a \mathrm{d}r, \tag{2}$$

where r is the local radius of the mid point of the annulus, U_∞ is the free stream wind velocity far in front of the rotor, Ω is the rotational velocity of the rotor, dr is the width of the annulus, and ρ is the density of air. They can also be expressed through blade element theory as

$$\mathrm{d}Q = N_\mathrm{b} \frac{1}{2} \rho U_\infty^2 (C_\mathrm{l} \sin\phi - C_\mathrm{d} \cos\phi) c r \mathrm{d}r, \tag{3}$$

$$\mathrm{d}T = N_\mathrm{b} \frac{1}{2} \rho U_\infty^2 (C_\mathrm{l} \cos\phi + C_\mathrm{d} \sin\phi) c \mathrm{d}r, \tag{4}$$

where N_b is the number of blades, C_l and C_d are the airfoil lift and drag coefficients (these values are often obtained experimentally or numerically and pulled from an airfoil lookup table based on the airfoil angle of attack), and c is the chord length of the airfoil. A derivation of these expressions can be found in Hansen's *Aerodynamics of Wind Turbines* [15].

The relative inflow angle of the wind velocity incident on the airfoil (ϕ) can be expressed as a function of the axial and angular induction factors a and a' which generally describe how much the incoming flow is decelerated by the rotor. This allows the two sets of equations for the torque and thrust contributions of the rotor annulus to be treated as a system of equations and solved via iteration for the variables a and a'. Once solved, the thrust and torque contributions of each annulus can be summed to determine the rotor-wide thrust and torque.

A variety of empirical corrections are used to augment this basic BEMT formulation. The corrections explored in this work are briefly described below.

The basic BEMT formulation assumes an infinite number of blades, and does not account for vortices shed by the blade tip or by the blade near the hub. A hub and tip loss model attempts to correct for these assumptions. We use the expression formulated by Prandtl [16] as implemented in the AeroDyn theory manual [8].

Glauert's correction is used for states in which the axial induction factor is large (greater than about 0.4). An empirical expression is used when the normal BEMT method predicts an axial induction factor over this critical value. The correction accounts for an increase in thrust for large induction factors where momentum theory nonphysically predicts the thrust to decrease. Here we use a modification of the original Glauert correction [17], which avoids numerical instabilities when combined with the hub-tip loss model described above. This modification was developed by Buhl [18] and is again presented in the Aerodyn theory manual [8].

Dynamic inflow corrections have been developed to account for the non-instantaneous change in wake dynamics behind the rotor as the upstream conditions change. Originally validated for fast blade pitch changes, they have been applied by multiple authors to analyze platform motion [19, 20]. In this work we examine two dynamic inflow corrections, the Stig ∅ye correction [21], and the Pitt Peters correction [22].

The Stig ∅ye method replaces the quasi-steady induction factor found through classical BEM at a time t with a new induction factor by passing it through two differential equation filters

$$y + \tau_1 \frac{\mathrm{d}y}{\mathrm{d}t} = U_0 + k\tau_1 \frac{\mathrm{d}U_0}{\mathrm{d}t}, \tag{5}$$

$$U_{0,\mathrm{adj}} + \tau_2 \frac{\mathrm{d}z}{\mathrm{d}t} = y, \tag{6}$$

where k is an empirically fitted constant = 0.6, U_0 is the initial induced velocity at the rotor plane, $U_{0,\mathrm{adj}}$ is the final, adjusted induced velocity, and y is an intermediate variable. The two time constants τ_1 and τ_2 are based on the rotor geometry. These filters model the delay between the upstream change in flow conditions and the downstream wake conditions and forces experienced by the rotor. The ∅ye model stems from a free vortex wake analysis of wind turbine rotor [23, 24] assuming constant uniform circulation, an infinite number of blades, cylindrical wake shape, and a finite tip speed ratio.

The Pitt Peters correction alters the momentum theory thrust equation with an additional added mass term which accounts for the additional inertial thrust required to accelerate the working fluid as the flow changes. Thrust contribution from each annulus becomes

$$\mathrm{d}T = 2\rho U_0(U_\infty - U_0)\mathrm{d}A + \mathrm{d}M_\mathrm{a}\frac{\mathrm{d}U_0}{\mathrm{d}t}, \tag{7}$$

where $\mathrm{d}A$ is the area of the annulus, and $\mathrm{d}M_\mathrm{a}$ is the axial added mass of a solid disk of the working fluid.

If desired, the BEMT equations can be altered to analyze each turbine blade individually. Single blade modeling allows for application of different relative velocities across each blade in rotational motion types where the platform induced velocity experienced by each blade section is a function of azimuthal position as well as annulus. Both the blade element and momentum equations are split to consider a single blade and third of an annulus, and the system of equations is solved separately for each blade.

To simulate the effect of a prescribed platform motion, the platform, tower, and rotor are assumed to be rigid. Sinusoidal functions prescribing the platform motion in surge are selected so that displacement at the rotor hub is

$$X_\mathrm{x} = A_\mathrm{x}\cos(\omega_\mathrm{x} t), \tag{8}$$

where A_x is the motion amplitude and ω_x is the motion frequency. The adjusted free stream velocity at each time step becomes

$$U_{\infty,\mathrm{adj}} = U_\infty * \cos(\theta_\mathrm{avg}) + \frac{\mathrm{d}X_\mathrm{x}}{\mathrm{d}t}. \tag{9}$$

The term $\cos(\theta_\mathrm{avg})$ is added to account for the mean platform pitch angle (θ_avg) which occurs in many operating states.

1	Classic	Classic BEMT
2	Single Blade	BEMT, Single Blade (SB) Modeling
3	Prandtl	BEMT, Hub-Tip Loss (HT) Correction
4	Prandlt Glauert	BEMT, HT, Glauert (G) Correction
5	Stig ∅ye	BEMT, HT, G, Stig ∅ye
6	Pitt-Peters	BEMT, HT, G, Pitt-Peters

TABLE 1: DESCRIPTION OF BEMT METHODS TESTED

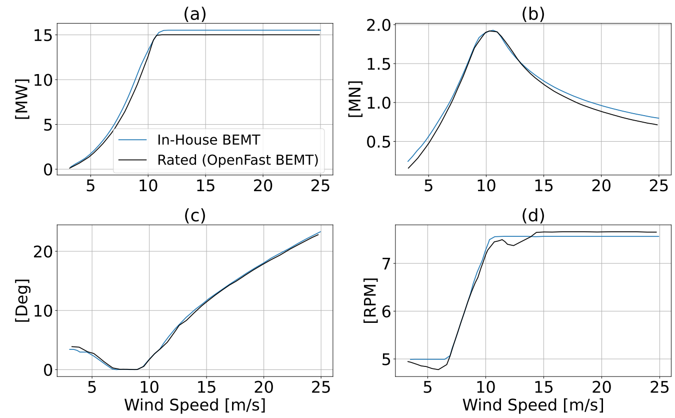

FIGURE 1: POWER (A) AND THRUST (B) CURVES PREDICTED BY IN-HOUSE BEMT CODE COUPLED WITH ROSCO VERSUS THE RATED VALUES IN THE IEA 15 MW DEFINITION DOCUMENT WHICH ARE COMPUTED WITH OPENFAST AND ROSCO, AS WELL AS THE BLADE PITCH (C) AND ROTOR SPEED (D) OUTPUTS FROM THE ROSCO CONTROLLER.

In order to validate the various BEMT corrections described above, five implementations of the in-house BEMT solver were created. Each implementation includes additional correction methods. The corrections included in each version of the model are described in Table 1.

3. VERIFICATION

The in-house BEMT code was compared to power and thrust curves for the IEA 15 MW reference wind turbine which are available in the reference wind turbine and control software technical definition documents [25, 26]. These performance curves were simulated with OpenFast and the NREL ROSCO controller. Comparisons of the reference curves with an in-house BEMT implementation with Prandtl's and Glauert's corrections are shown in Figure 1. The in-house BEMT solver predicts power coefficient with 4.4 % difference and thrust coefficient with 2.3 % difference to OpenFast at the rated wind speed. The two models are very similar at below rated wind speeds, but diverge slightly at high wind speeds. Above the rated wind speed the in-house solver predicts higher power and thrust than OpenFast. This is likely due to the reference curves inclusion of flexible blade and tower effects while the in-house BEMT model assumes a rigid tower and blades. Even at the cut out wind speed the discrepancy between the two aerodynamic solvers is less than four percent in power coefficient and less than ten percent in thrust coefficient.

4. VALIDATING BLADE ELEMENT MOMENTUM THEORY FOR PRESCRIBED PLATFORM MOTION

To validate and characterize BEMT's ability to predict mean and fluctuating rotor integrated parameters we conducted three validation studies. The first validation study compared the in-house BEMT solver to blade resolved Reynolds averaged Navier-Stokes computational fluid dynamics (RANS-CFD) simulations of a 20 m diameter tidal turbine conducted by Bin Osman [27]. Although we are primarily interested in the performance of floating wind, the physics governing blade element momentum analysis of tidal and wind turbines are highly similar. In addition, the Bin Osman data is of high quality and was readily available. For these reasons, we proceed with validation of our BEMT method against the results of Bin Osman as one of our three validation studies. Additionally, using one tidal turbine case allows for comparison of the Pitt Peters method with varying fluid densities in the added mass term. We expect added mass effects to be of greater significance for the tidal turbine due to the large fluid density, and thus the Pitt Peters correction may have varying efficacy for a tidal turbine compared to a wind turbine. Ten surge-motion cases were studied in which the amplitude and frequency of the platform motion as well as the rotor tip speed ratio were varied with a constant free stream velocity. The tidal turbine was originally developed by Schluntz and Willden [28] and modified by Wimshurst and Willden [29].

A time series of one period of platform motion for two surge motion cases is shown in Figure 2. For the platform motion of 0.25 m amplitude, the BEMT methods accurately model the sinusoidal response of the power and thrust coefficient to the prescribed harmonic motion. A similar sinusoidal response is predicted by the RANS-CFD. The implementation with Prandtl's hub tip loss and Glauerts turbulent wake method performs the best relative to the high fidelity model in both C_P and C_T prediction. However, for the more extreme platform motion of 1.0 m amplitude, the blade resolved RANS-CFD predicts a non-sinusoidal response due to flow separation and span wise flow anomalies that the BEMT is unable to model. In extreme cases the accuracy of the BEMT model degrades as stall, flow recirculation, and viscous wake effects become significant. However, this type of motion is unrealistic for turbine operation (power and thrust coefficient reach zero during the motion cycle).

The various BEMT methods' predictions of the average power and thrust coefficient over a period of platform motion for all ten test cases conducted by Bin Osman, as well as the percent difference to that predicted by the RANS-CFD, are shown in Figures 3 and 4. The predictions for the amplitude of the power and thrust coefficient are shown in Figures 5 and 6. All cases are plotted against the normalized induced velocity due to platform motion $\Delta U^* = \Delta U_{\max}/U_{\text{rated}}$.

In Figures 3 through 6 a subset of test cases vary the rotor rotational speed, but not the platform motion. This affects performance but not motion induced inflow velocity. As such, there can be two data points for single value of motion induced inflow velocity. In the prediction of average power and thrust coefficient there is a clear trend between normalized platform induced velocity and error relative to the higher fidelity RANS-CFD. The BEMT methods 4 (with Prandtl's and Glauert's correction) and

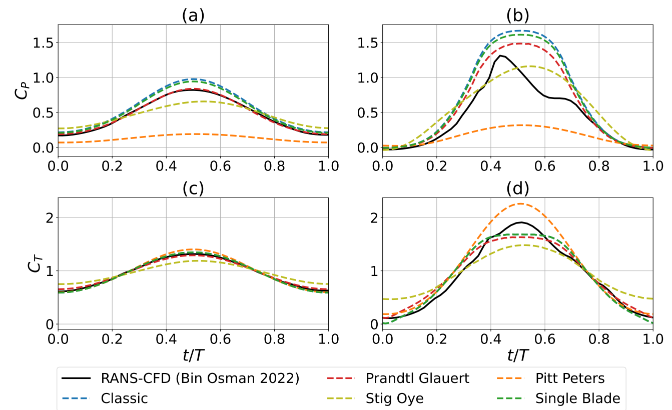

FIGURE 2: TIME SERIES OF CP FOR SURGE MOTION AT A=0.25 M, F=0.14 HZ (A), CP FOR SURGE MOTION AT A=1.0 M, F=0.14 HZ (B), CT FOR SURGE MOTION AT A=0.25 M, F=0.14 HZ (C), AND CT FOR SURGE MOTION AT A=1.0 M, F=0.14 HZ (D).

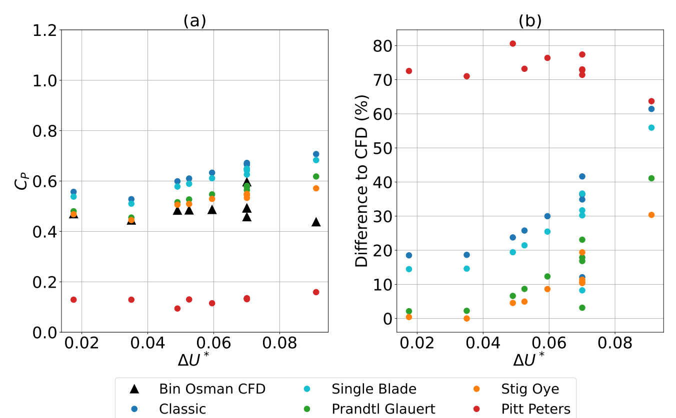

FIGURE 3: THE AVERAGE POWER COEFFICIENT PREDICTED BY THE BLADE RESOLVED RANS-CFD PRESENTED BY BIN OSMAN 2022 AND BY VARIOUS IMPLEMENTATIONS OF THE IN-HOUSE BEMT SOLVER (A) AND DIFFERENCE TO THE RANS-CFD (B).

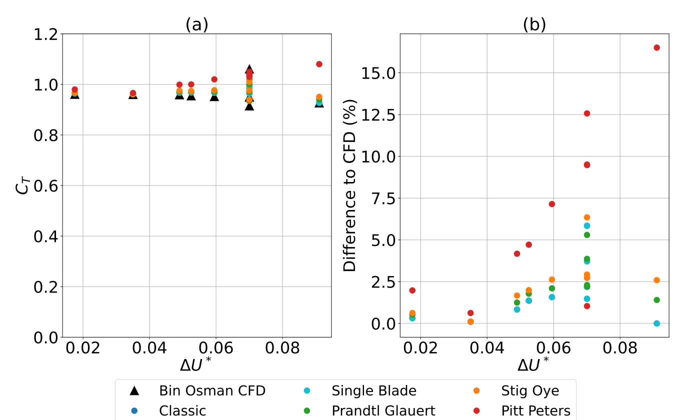

FIGURE 4: THE AVERAGE THRUST COEFFICIENT PREDICTED BY THE BLADE RESOLVED RANS-CFD PRESENTED BY BIN OSMAN 2022 AND BY VARIOUS IMPLEMENTATIONS OF THE IN-HOUSE BEMT SOLVER (A) AND DIFFERENCE TO THE RANS-CFD (B).

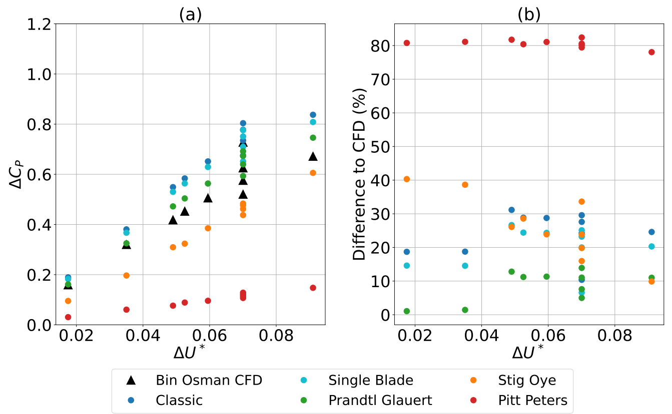

FIGURE 5: THE AMPLITUDE OF THE POWER COEFFICIENT PREDICTED BY THE BLADE RESOLVED RANS-CFD PRESENTED BY BIN OSMAN 2022 AND BY VARIOUS IMPLEMENTATIONS OF THE IN-HOUSE BEMT SOLVER (A) AND DIFFERENCE TO THE RANS-CFD (B).

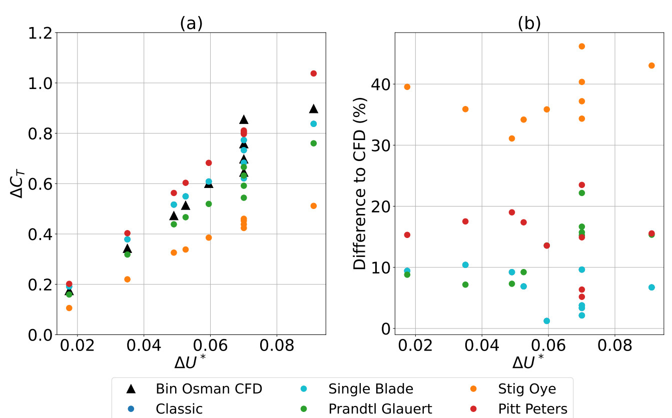

FIGURE 6: THE AMPLITUDE OF THE THRUST COEFFICIENT PREDICTED BY THE BLADE RESOLVED RANS-CFD PRESENTED BY BIN OSMAN 2022 AND BY VARIOUS IMPLEMENTATIONS OF THE IN-HOUSE BEMT SOLVER (A) AND DIFFERENCE TO THE RANS-CFD (B).

5 (with Prandtl's, Glauert's, and the Stig ∅ye correction) perform the best, achieving approximately 3 % root mean square error (RMSE) where $RMSE = \sqrt{\frac{1}{n}\sum_{i=1}^{n}\left(\frac{x_i-\hat{x}_i}{x_i}\right)^2}$ in thrust coefficient prediction and 8 % in power coefficient relative to the RANS-CFD. For prediction of the amplitude of thrust and power coefficient there is not a clear relationship between error and platform induced velocity. The single blade and Prandtl - Glauert implementations (methods 2 and 4) perform the best achieving between 4 and 10 % RMSE relative to the RANS-CFD depending on motion induced velocity. A discrepancy to the higher fidelity model of less than 10 % is considered to be acceptable in this case, given the four to five orders of magnitude decrease in computational expense granted by the BEMT method. In addition, we see the steady BEMT method's ability to predict the mean and fluctuating components of power and thrust with an acceptable and similar error for all parameters. The Pitt Peters correction is shown to severely under predict turbine torque. We would expect the additional added mass term to be especially important for the tidal case, but find that it is detrimental to accuracy compared to the results of Bin Osman presented here.

The next validation study consisted of a comparison with an experimental model designed to replicate the rotor thrust characteristics of the DTU 10 MW reference wind turbine designed by Bak et al. [30]. The experimental results were obtained from a 1:148 scale model designed by Taruffi et al. [31] utilizing an airfoil design presented in Fontanella et al. 2023 [32]. The scale turbine was operated in a wind tunnel while the turbine base was mechanically actuated to simulate platform motion.

The blade geometry of the Taruffi et al. turbine is not geometrically scaled from the full DTU 10 MW RWT geometry. Additionally, the airfoil utilized in the experimental model is different from those used in the full scale turbine. The Taruffi et al. model is performance scaled, and the experiment does not aim to match Reynolds numbers between the experimental and full scale blades. The experimental blade geometry is instead tuned to preserve the rotor thrust coefficient from the full scale turbine for a wind speed reduction factor of three. We compare the variation in thrust predicted by the Taruffi et al. experimental model to that predicted by BEMT analyzing the same experimental scale geometry for seven surge-type motion cases. Throughout these cases the maximum velocity induced by platform motion is kept constant. The amplitude of rotor thrust coefficient for each case as predicted by the various BEMT implementations and by the experimental model is shown in Figure 7. The amplitude of thrust coefficient is normalized by the rated value, and frequency is represented as rotor reduced frequency where $F_r = \frac{fR}{U_\infty}$, f is the motion frequency, and R is the rotor radius.

The steady BEMT implementations (classical, single blade, and Prandtl's and Glauert's correction) do not exhibit a frequency dependence, so they predict the same thrust fluctuation for all cases where the normalized platform-induced velocity is constant. The Stig ∅ye method does exhibit frequency dependence, however for this range of frequencies and rotor geometry the variation is very minor (magnitude of 10^{-3} C_T). In contrast the Pitt Peters method displays a strong frequency dependence. However, the accuracy of the Pitt Peters method relative to the experimen-

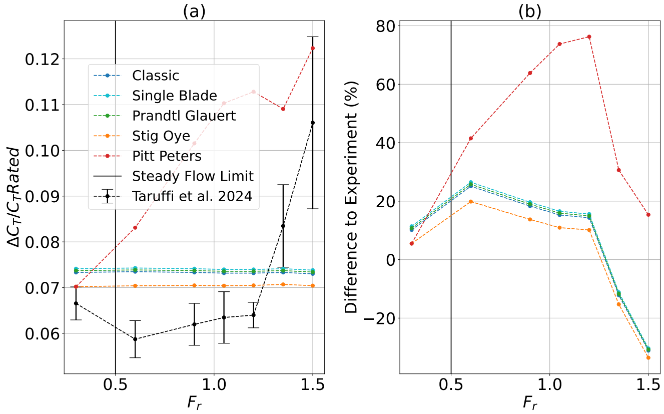

FIGURE 7: NORMALIZED AMPLITUDE OF THRUST COEFFICIENT OVER A SINGLE PERIOD OF PLATFORM MOTION AS A FUNCTION OF ROTOR REDUCED FREQUENCY (A) AND THE PERCENT DIFFERENCE OF THE BEMT METHODS RELATIVE TO THE EXPERIMENTAL RESULTS OF TARUFFI ET AL. (B).

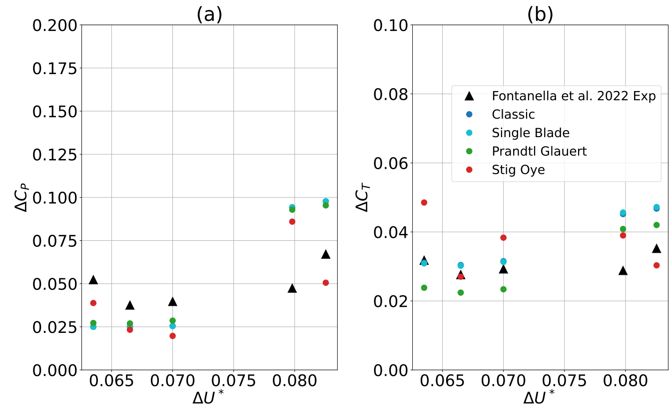

FIGURE 8: THE AMPLITUDE OF POWER COEFFICIENT (A) AND THRUST COEFFICIENT (B) PREDICTED BY THE BEMT IMPLEMENTATIONS AND THE EXPERIMENTAL MODEL OF FONTANELLA ET AL. 2022.

tal results is very poor for reduced frequencies between 0.6 and 1.3. The Pitt Peters method does not demonstrate better accuracy for this low density working fluid case compared to the Bin Osman cases. The other BEMT methods are relatively tightly grouped ranging from 10 to 31 absolute percent difference to the experimental results.

Fontanella et al. 2021 [33] determined through experimental testing that the airfoil utilized in this campaign would begin to experience unsteady local flow characteristics in surge motion with rotor reduced frequency greater than one half. We see the best accuracy of the BEMT methods below this limit (5.5 to 11 % difference to experimental results). The range of frequencies tested here is significantly above the natural frequencies of representative floating platforms. The UMaine Volturnus floater has a natural frequency of 0.007 Hz in surge and 0.036 Hz in pitch [34]). For reference, motion at the surge natural frequency would result in a reduced frequency of 0.08. However, platform motion will also occur at wave frequencies significantly higher than the natural frequency, so it is still useful to quantify BEMT error in this range. A representative wave frequency identified by Fontanella et al. 2024 was 0.111 Hz [35]. We aim to characterize the limit of BEMT applicability, so testing high frequency motion is necessary to determine the BEMT method's accuracy beyond steady flow limits.

A final validation study was conducted comparing the BEMT implementations to an additional experimental model. Fontanella et al. [36] conducted wind tunnel testing of a 1:100 scale model of the IEA 15 MW RWT [25] using a similar performance scaling methodology as Taruffi et al. [31]. In this case the blade geometry was tuned to preserve the span-wise lift distribution for a wind speed reduction factor of three. The experimental model was then operated while actuators at its base prescribed platform motion in each of its six degrees of freedom individually.

We compare the BEMT prediction of power and thrust amplitude to the five cases in surge-type motion analyzed by Fontanella et al. In each case the rotor aerodynamic torque and thrust are measured via force gauges at the rotor hub during the same platform motion both with and without the wind tunnel active. The force measured during the platform motion without wind is subtracted from the time series with the wind tunnel active. The resultant time series of thrust and torque is then treated using a Fourier transform. The magnitude at the prescribed platform motion frequency is taken to be the torque and thrust amplitude of the turbine. This process is described in Fontanella et al. 2022 [36].

The amplitude of the power and thrust coefficient for the experimental turbine as a function of ΔU^* are shown in Figure 8. The steady BEMT methods achieve 2 to 24 % difference to the experimental results in thrust amplitude for the three cases with ΔU^* less than 0.075. However, for large ΔU^* the BEMT method's accuracy relative to the experimental results shows poor agreement (19 to 58 % difference for the steady BEMT methods in thrust amplitude). For these high ΔU^* cases, the steady BEMT methods generally over-predict the experimental results. It is possible that this is due to the magnitude of the aerodynamic response from the experimental data being taken only at the excitation frequency. The actual response may leak into frequencies slightly smaller or larger than the excitation frequency, and thus the measured experimental result may be an under-prediction.

5. ROTOR RESPONSE TO PRESCRIBED PLATFORM MOTION

To characterize the effect of platform motion on turbine performance during realistic operation, we utilize the in-house BEMT solver with Prandtl's and Glauert's corrections and the NREL ROSCO controller to generate "motion adjusted" power and thrust curves for the IEA 15 MW reference wind turbine [25]. A platform motion is prescribed, and the BEMT solver coupled with ROSCO simulates seven periods of platform motion for each wind speed across the operational range. The average power and thrust over the last period of motion are then recorded. The adjusted curves are compared to a "static" curve with no platform motion. The static curve describes the turbine's ideal power performance and thrust loading across its operational wind speed range. To the best of the authors' knowledge, platform motion

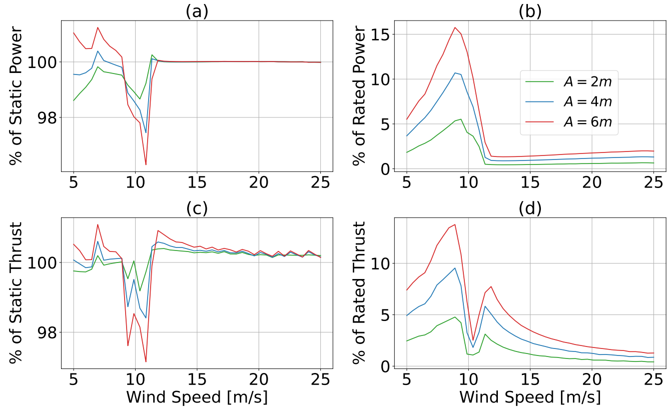

FIGURE 9: NORMALIZED AVERAGE COMPONENT OF POWER (A), FLUCTUATING COMPONENT OF POWER (B), AVERAGE COMPONENT OF THRUST (C), AND FLUCTUATING COMPONENT OF THRUST (D) AS A FUNCTION OF WIND SPEED IN PRESCRIBED SURGE MOTION AT 0.007 HZ.

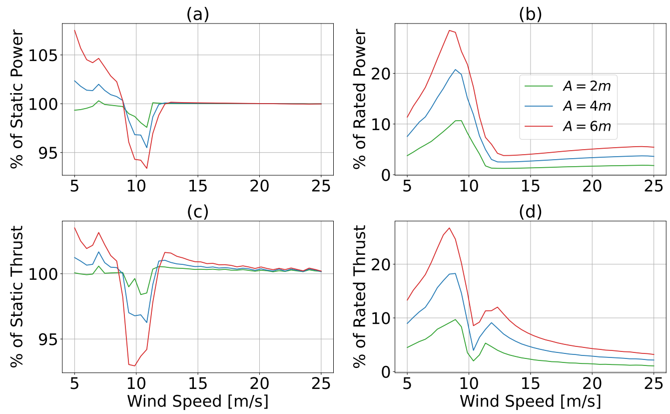

FIGURE 10: NORMALIZED AVERAGE COMPONENT OF POWER (A), FLUCTUATING COMPONENT OF POWER (B), AVERAGE COMPONENT OF THRUST (C), AND FLUCTUATING COMPONENT OF THRUST (D) AS A FUNCTION OF WIND SPEED IN PRESCRIBED SURGE MOTION AT 0.012 HZ.

adjusted performance curves for the IEA 15 MW RWT have not been previously published.

We examine the prescribed surge motion of the platform at the natural surge frequency of the VolturnUS-S reference platform [34] (0.007 Hz), the natural surge frequency of the WindCrete Spar reference platform [37] (0.012 Hz), as well as a representative wave frequency defined by Fontanella et al. 2024 for a prospective FOWT site in the Mediterranean Sea [35] (0.111 Hz). At each frequency the amplitude of motion is also varied between 5 and 10 m for the two low frequencies and 2 and 6 m for the wave frequency. For all test cases a constant mean platform pitch of four degrees (backward tilt due to turbine thrust) is assumed. This angle is typical for operational conditions and slightly decreases average power capture. The average and fluctuating components of turbine power and thrust during surge motion at the three frequencies of interest are shown in Figures 9, 10, and 11.

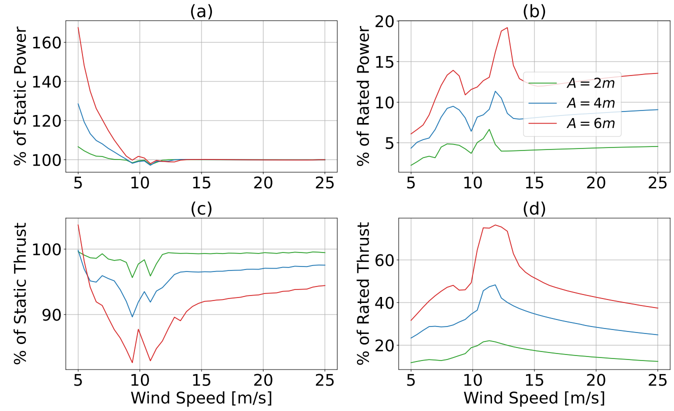

FIGURE 11: NORMALIZED AVERAGE COMPONENT OF POWER (A), FLUCTUATING COMPONENT OF POWER (B), AVERAGE COMPONENT OF THRUST (C), AND FLUCTUATING COMPONENT OF THRUST (D) AS A FUNCTION OF WIND SPEED IN PRESCRIBED SURGE MOTION AT 0.111 HZ.

We find that the effect of platform motion scales with $\frac{U_{induced}}{U_\infty}$, where a larger motion induced velocity causes a larger effect on power and thrust. The specific effect of motion varies based on the wind speed regime and resulting controller response.

In the below-rated region (between 3 m/s and about 9 m/s) average power capture is increased by up to to 60% at 5 m/s and up to 15% at 8 m/s compared to the static turbine benchmark. This increase in average power capture over a platform motion cycle is due to the cubic relation between wind speed and power. The increase in turbine power production during the upwind motion portion of the oscillation outweighs the decrease in power production during the downwind motion portion of oscillation due to the cubic scaling between power and wind speed. In this same region the average thrust increases up to 7 % difference from static. This suggests an increase in turbine performance compared to static (better power capture, with the same or similar blade loads) under a prescribed platform motion when wind speed is low.

This finding is qualified by the observation made previously that platform motion causes a variance in rotor torque and thrust which has important implications for component loading. The amplitude of both power and thrust increases up to 30% of rated in the low frequency cases and 70% for the high frequency case. In the below rated region the varying loads will not exceed the rated torque and thrust, so it is unlikely that an unsafe load will be encountered. However, load cycling can have significant effects on component fatigue. This is not explored further here, but must be taken into consideration in FOWT design and is left for future work.

Conversely, power capture is decreased (up to 6% difference to static) close to the rated wind speed (9 m/s to 15 m/s). In this region thrust is also decreased by up to 8% compared to static. This decrease is due to the turbine controller which caps the power generated at its rated value. This limiting is done to avoid above rated loads when the platform motion induces a wind speed above rated. However, the turbine cannot capture the rated power when the induced wind speed is below rated, causing a decrease

Study	Parameter	C	SB	PG	S∅	PP
1	C_P	14.8	12.9	8.19	6.80	36.1
1	C_T	2.78	2.78	2.89	3.18	7.83
1	ΔC_P	12.0	9.89	4.41	12.0	40.0
1	ΔC_T	3.18	3.17	8.66	23.0	8.30
2	ΔC_T	18.1	18.7	18.4	15.6	43.8
3	ΔC_P	53.1	53.1	48.4	44.0	N/A
3	ΔC_T	21.9	22.2	25.0	27.0	N/A

TABLE 2: ROOT MEAN SQUARE ERROR, EXPRESSED AS PERCENTAGE, FOR EACH BEMT IMPLEMENTATION RELATIVE TO A HIGHER FIDELITY MODEL. THE BEMT METHODS ARE WRITTEN AS ABBREVIATIONS, WHERE C IS CLASSIC BEMT, SB IS SINGLE BLADE, PG IS PRANDTL-GLAUERT, S∅ IS STIG ∅YE, AND PP IS PITT PETERS.

in average power capture over the motion cycle. This behavior is dependent on the specific controller used, but representative of many wind turbine controllers.

Once the wind speed increases sufficiently, the platform motion never causes motion-induced wind speed to drop below rated. At this point power capture and thrust return to their rated, or static turbine, values. This return to static operation occurs when the free stream velocity is greater than the sum of the rated wind speed and maximum velocity induced by the platform motion. As such, it is dependent on the specific platform motion amplitude and frequency.

The effect of a prescribed platform motion on turbine performance can thus be generally categorized by the turbine's three operational regions. Motion is possibly beneficial in region one (below rated wind speed), clearly detrimental in region two (near rated wind speed), and possibly unimportant in region three (significantly above rated wind speed). These results are in line with the findings of Cottura et al. 2021 [13], and suggest that platform motion can increase power capture in limited conditions.

6. DISCUSSION AND CONCLUSIONS

The work presented here first demonstrates the suitability of BEMT for low-order analysis of floating wind. In order to quantify the accuracy of the BEMT method, we compute the root mean square error of each parameter studied in the three validation studies for each BEMT implementation relative to the higher-fidelity model. The results are shown in Table 2. The Pitt Peters method was not examined in validation Study 3 due to its large error in the prior two studies. Additionally, the large error in the fluctuation of power coefficient in validation Study 3 is likely due to issues in the frequency domain data processing described previously. Omitting the comparison of power coefficient from Study 3, we see a range in BEMT discrepancy to higher fidelity models between 3 and 27 %.

Comparing the various BEMT implementations to each other, we see that for the prediction of the mean power and thrust coefficients the Prandtl-Glauert and the Stig ∅ye implementation perform the best with under 10 % RMSE. However, for the amplitude of power and thrust coefficient the addition of the Stig ∅ye model decreases the prediction accuracy for three of the five comparisons (ΔC_P Study 1, ΔC_T Study 1, and ΔC_T Study 3). The added efficacy offered by the Stig ∅ye model is thus uncertain. The other dynamic inflow model, the Pitt Peters method, vastly under performs all of the other implementations.

The poor performance of the dynamic inflow models relative to the steady BEMT methods, is likely due to a fundamental difference between platform motion and the case studies these dynamic models were derived under. The Stig ∅ye method has only been validated for instantaneous changes in blade pitch or rotor speed after which the rotor was allowed to return to steady state [38, 39]. The Pitt Peters method was derived as an approximation of an instantaneous change in thrust coefficient at the rotor plane [22]. The Stig ∅ye and Pitt Peters methods were derived to account for instantaneous changes in induced velocity or variations in rotor axial force due to these changes. However, Snel and Schepers [40] show through experimental wind tunnel results that although the induction factor changes with variations in free stream velocity, the induced velocity is relatively unaffected. As such, the underlying mechanism in dynamic inflow effects that are modeled by methods such as ∅ye and Pitt Peters are fundamentally different than the dynamics caused by steady changes in free stream velocity during events such as low frequency, harmonic, platform motion.

These observations lead to the conclusion that there is no clear theoretical indication that dynamic inflow methods could improve the accuracy of quasi-steady BEMT methods for the case of harmonic platform motion. This is supported by the data presented here, which indicates that the benefit in accuracy from dynamic inflow modeling is uncertain. Additionally, these findings are in line with the results of Papi et al. [14] and Bergua et al. [41] who find that dynamic corrections for BEMT do not increase accuracy relative to higher fidelity models for cases that do not include oscillations of blade pitch and rotor speed.

In addition to the comparison between BEMT methods, we are able to characterize the effective range of BEMT analysis based on motion frequency or platform motion induced velocity. From validation against the DTU 10 MW experimental model, we see a clear indication that the steady flow limit of $f_\mathrm{r} = 0.5$ proposed by Fontanella et al 2021, does demarcate a significant decrease in BEMT accuracy relative to the experimental model. As expected, BEMT is less accurate in unsteady flow conditions.

The applicability of BEMT can also be determined through the normalized platform induced velocity. The accuracy of the BEMT Method 4, with Prandtl's and Glauert's corrections, decreases as ΔU^* increases. In Study 1 for a $\Delta U^* < 0.07$, the percent difference was under 10 % for ΔC_T, 12 % for ΔC_P, 5 % for C_T, and 20 % for C_P. In comparison to the experimental model of the IEA 15 MW turbine, the BEMT accuracy also deteriorates for $\Delta U^* > 0.07$. A limit of $\Delta U^* = 0.07$ would correspond to a 0.7 Hz motion at 1 m amplitude or a 0.07 Hz motion at 10 m amplitude for rated wind speeds. This includes much of the range of surge motion expected in operational conditions. In addition, these validation results indicate sufficient accuracy for high-level analysis in thrust and amplitude of thrust prediction which will lead to better modeling of the induced motion of the coupled turbine, platform system. Single blade modeling does not significantly affect BEMT accuracy, but may be important for coupled aero-hydro dynamic modeling. BEMT's sufficient accuracy for high-level analysis, coupled with its low computational load makes it a reasonable tool for time domain analysis over large sample periods (many hours or days). Through these long time domain analyses we can better predict long-term FOWT performance.

The BEMT method was then applied to generate "motion adjusted" turbine performance curves. Static performance curves are often used to estimate the suitability of a potential wind farm and estimate long-term power production [42]. However, motion's effect on performance is not accounted for, and motion adjusted performance curves of the average and fluctuating components of power and thrust for the IEA 15 MW RWT have not previously been published. With this low fidelity BEMT method we demonstrate a way to account for platform motion in turbine power and thrust curves and increase the accuracy of long-term turbine performance prediction. However, it is important to note that the prescribed harmonic motions used here are only representative of possible motion responses. Through fully coupled aero-hydrodynamic modeling, we can better predict platform motion and turbine response, but that is left for future work.

Using the BEMT method to predict the effect of a prescribed platform motion across the operational wind speed spectrum of a turbine, we find that the effect of motion is highly dependent on wind speed region. Platform motion is shown to be the most detrimental to power capture around rated wind speed, causing up to a 7 % decrease in average power capture over a motion cycle. However, the average thrust experienced by the turbine is also decreased by up to 15 % in this region. It is important to note that the turbine response near rated wind speeds is heavily influenced by controller design. The results presented here are produced with the NREL ROSCO controller which is meant to be representative of industry standard control practices, but may not be representative of all wind turbine controllers. At below rated wind speeds platform motion enhances power capture by up to 60 %, while it has little effect at high wind speeds.

These results suggest that platform motion could be beneficial to turbine operation in certain wind regimes. This raises the possibility of controller design that aims to damp motion near rated speeds, but that allows some motion at lower wind speeds. Additionally, depending on the predominant wind speeds of a potential turbine site, a platform or controller that decreases platform motion may be more or less important. In a site that almost always experiences very high wind speeds, platform motion is less important to turbine average power capture. This has important ramifications for site specific platform design or controller tuning.

We aim to explore wave and wind induced motion's effects further in future work through analysis of the FOWT as a coupled hydrodynamic and aerodynamic system. The BEMT model presented here will be used with a potential flow hydrodynamic solver to create a coupled model that maintains sufficient computational efficiency to conduct large-scale time domain simulations. Through long time domain simulation, the coupled model will be able to predict long-term performance of a FOWT through metrics such as annual energy production (AEP)

ACKNOWLEDGMENTS

We would like to thank the Oxford Environmental Fluid Mechanics group, as well as the Oxford Department of Engineering for making this work possible.

REFERENCES

[1] Edwards, E., Holcombe, A., Brown, S., Ransley, E, Hann, M. and Greaves, D. "Evolution of Floating Offshore Wind Platforms: A Review of At-Sea Devices." *Renewable and Sustainable Energy Reviews* Vol. 183 (2023).

[2] Edwards, E., Holcombe, A., Brown, S., Ransley, E., Hann, M. and Greaves, D. "Trends in floating offshore wind platforms: A review of early-stage devices." *Renewable and Sustainable Energy Reviews* (2024).

[3] Tran, T.T. and Kim, D.H. "A CFD study into the influence of unsteady interference on wind turbine surge motion." *Renewable Energy* Vol. 90 (2016).

[4] Sebastian, T. and Lackner, M.A. "Development of a free vortex wake method code for offshore floating wind turbines." *Renewable Energy* Vol. 46 (2012).

[5] Lee, H. and Lee, D.J. "Effects of platform motions on aerodynamic performance and unsteady wake evolution of a floating offshore wind turbine." *Renewable Energy* Vol. 143 (2019).

[6] Ramos-Garcia, N., Kontos, S., Pegalajar-Jurado, A., Horcas, S.G. and Bredmose, H. "Investigation of the floating IEA Wind 15 MW RWT using vortex methods Part I: Flow regimes and wake recovery." *Wind Energy* Vol. 25 (2021).

[7] Shaler, K., Anderson, B., Martines-Tossas, L.A., Branlard, E. and Johnson, N. "Comparison of free vortex wake and blade element momentum results against large-eddy simulation results for highly flexible turbines under challenging inflow conditions." *Wind Energy Science* (2023).

[8] Moriarty, P.J. and Hansen, A.C. "AeroDyn Theory Manual." Technical report no. US National Renewable Energy Laboratory. 2005.

[9] Ledoux, J., Riffo, S. and Salomon, J. "Analysis of the Blade Element Momentum Theory." *SIAM Journal on Applied Mathematics* Vol. 81 (2021).

[10] Apsley, D.D. and Stansby, P.K. "Unsteady thrust on an oscillating wind turbine: Comparison of blade-element momentum theory with actuator-line CFD." *Journal of Fluids and Structures* Vol. 98 (2020).

[11] Tran, T.T. and Kim, D. "The platform pitching motion of floating offshore wind turbine: A preliminary unsteady aerodynamic analysis." *Journal of Wind Engineering and Industrial Aerodynamics* Vol. 142 (2015).

[12] de Vaal, J.B., Hansen, M.O. and Moan, T. "Effect of wind turbine surge motion on rotor thrust and induced velocity." *Wind Energy* Vol. 17 (2014).

[13] Cottura, L., Caradonna, R., Novo, R., Ghigo, A., Bracco, G. and Mattiazzo, G. "Effect of Pitching Motion on Production in a OFWT." *Journal of Ocean Engineering and Marine Energy* (2022).

[14] Papi, F., Jonkman, J., Robertson, A. and Bianchini, A. "Going Beyond BEM with BEM: an Insight into Dynamic In-

flow Effects on Floating Wind Turbines [Preprint]." *Wind Energy Science Discussions* (2023).

[15] Hansen, M.O.L. *Aerodynamics of Wind Turbines*. Routledge (2015).

[16] Glauert, H. *Aerodynamic Theory*. Springer (1935).

[17] Glauert, H. "The Analysis of Experimental Results in the Windmill Brake and Vortex Ring States of an Airscrew." *ARCR R and M* (1926).

[18] M.L. Buhl, Jr. "A New Empirical Relationship between Thrust Coefficient and Induction Factor for the Turbulent Windmill State." Technical report no. National Renewable Energy Laboratory. 2005.

[19] Mancini, S., Boorsma, K., Schepers, G. and Savenije, F. "A comparison of dynamic inflow models for the blade element momentum method." *Wind Energy Science* Vol. 8 (2023).

[20] Ferreira, C., Yu, W., Sala, A. and Vire, A. "Dynamic inflow model for a floating horizontal axis wind turbine in surge motion." *Wind Energy Science* Vol. 7 (2022).

[21] Snel, H. and Schepers, J. G. "Joint investigation of dynamic inflow effects and implementation of an engineering method." Technical report no. Netherlands. 1995.

[22] Lupton, R. "Frequency-domain modelling of floating wind turbines." Ph.D. Thesis, University of Cambridge. 2014.

[23] Branlard, E. and Gaunaa, M. "Cylindrical vortex wake model: right cylinder." *Wind Energy* Vol. 18 (2015).

[24] Oye, S. "A Simple Vortex Model of a Turbine Rotor." *Proc. of the third IEA Symposium on the Aerodynamics of Wind Turbines, ETSU* (1990).

[25] Gaertner, E., Rinker, J., Sethuraman, L., Zahle, F., Anderson, B., Barter, G.E., Abbas, N.J., Meng, F., Bortolotti, P., Skrzypinski, W., Scott, G.N., Feil, R., Bredmose, H., Dykes, K., Shields, M., Allen, C. and Viselli, A. "IEA Wind TCP Task 37: Definition of the IEA 15-Megawatt Offshore Reference Wind Turbine." (2020)DOI 10.2172/1603478. URL https://www.osti.gov/biblio/1603478.

[26] Abbas, N., Zalkind, D., Pao, L. and Wright, A. "A Reference Open-Source Controller for Fixed and Floating Offshore Wind Turbines." *Wind Energy Science Discussions* Vol. 2021 (2021): pp. 1–33. DOI 10.5194/wes-2021-19. URL https://wes.copernicus.org/preprints/wes-2021-19/.

[27] Bin Osman, M.H. "Unsteady loading on floating horizontal axis tidal turbine." Ph.D. Thesis, University of Oxford. 2022.

[28] Schluntz, J. and Willden, R.H.J. "The effect of blockage on tidal turbine rotor design and performance." *Renewable Energy* (2015).

[29] Wimshurst, A. and Willden, R.H.J. "Tidal power extracttion on a streamwise bed slope." *Ocean Engineering* (2016).

[30] Bak, C., Zahle, F., Bitsche, R., Kim, T., Yde, A., Henriksen, L.C., Hansen, M.H., Blasques, J.P.A.A, Gaunaa, M. and Natarajan, A. "The DTU 10 MW Reference Wind Turbine." Technical report no. Danish Technical University. 2013.

[31] Taruffi, F., Novais, F. and Vire, A. "An experimental study on the aerodynamic loads of a floating offshore wind turbine under imposed motions." *Wind Energ. Sci* (2024)DOI https://doi.org/10.5194/wes-9-343-2024.

[32] Fontanella, A., Da Pre, G. and Belloli, M. "Integrated Design and Experimental Validation of a Fixed-Pitch Rotor for Wind Tunnel Testing." *Energies 16, 2205* (2023)DOI https://doi.org/10.3390/en16052205.

[33] Fontanella, A., Bayati, I., Mikkelsen, R. and Zasso, M. Belloliand A. "UNAFLOW: a holistic wind tunnel experiment about the aerodynamic response of floating wind turbines under imposed surge motion." *Wind Energy Science* (2021).

[34] Allen, C., Viselli, A., Dagher, H., Goupee, A., Gaertner, E., Abbas, N., M.Hall and Barter, G. "Definition of the UMaine VolturnUS-S Reference Platform Developed for the IEA Wind 15-Megawatt Offshore Reference Wind Turbine." (2020)DOI 10.2172/1603478. URL https://www.nrel.gov/docs/fy20osti/76773.pdf.

[35] Fontanella, A., Colpani, G., De Pascali, M., Muggiasca, S. and Belloli, M. "Assessing the impact of waves and platform dynamics on floating wind-turbine energy production." *Wind Energy Science* (2024).

[36] Fontanella, A., Facchinetti, A., Carlo, S. Di and Belloli, M. "Wind tunnel investigation of the aerodynaic response of two 15 MW floating wind turbines." *Wind Energy Science* (2022).

[37] Mahfouz, M., Salari, M., Hernandez, S., Vigara, F., Molins, C., Trubat, P., H.Bredmose and Pegalajar-Jurado, A. "Public design and FAST model of the two 15MW float-turbine concepts." Technical report no. Corewind. 2020.

[38] Oye, S. "Fast pitch step experiments in a wind tunnel and comparison with computational methods." *Proceedings on the 1996 European Union Wind Energy Conference* (1996).

[39] Schepers, Jan G. "Engineering models in wind energy aerodynamics." Ph.D. Thesis, Technical University of Delft. 2012.

[40] Snel, H. and Schepers, J.G. "JOULE1: Joint investigation of Dynamic Inflow Effects and Implementation of an Engineering Method." Technical report no. Energy Research Centre of the Netherlands, ECN. 1994.

[41] Bergua, R., Robertson, A., Jonkman, J., Branlard, E., Fontanella, A., Belloli, M., Schito, P., Zasso, A., Persico, G., Sanvito, A., Amet, E., Brun, C., Campaña-Alonso, G., Martín-San-Román, R., Cai, R., Cai, J., Qian, Q., Maoshi, W., Beardsell, A., Pirrung, G., Ramos-García, N., Shi, W., Fu, J., Corniglion, R., Lovera, A., Galván, J., Nygaard, T. Anders, dos Santos, C. Renan, Gilbert, P., Joulin, P., Blondel, F., Frickel, E., Chen, P., Hu, Z., Boisard, R., Yilmazlar, K., Croce, A., Harnois, V., Zhang, L., Li, Y., Aristondo, A., Alonso, I. Mendikoa, Mancini, S., Boorsma, K., Savenije, F., Marten, D., Soto-Valle, R., Schulz, C., Netzband, S., Bianchini, A., Papi, F, Cioni, S., Trubat, P., Alarcon, D., Molins, C., Cormier, M., Brüker, K., Lutz, T., Xiao, Q., Deng, Z., Haudin, F. and Goveas, A. "OC6 project Phase III: validation of the aerodynamic loading on a wind turbine rotor undergoing large motion caused by a floating support structure." *Wind Energy Science* (2023).

[42] Diaz, H. and Soares, C. Guedes. "An integrated GIS approach for site selection of floating offshore wind farms in the Atlantic continental European coastline." *Sustainable Energy Reviews* Vol. 134 (2020).